5-7-2011

Characterization and Implementation of Low Intensity Pulsed Ultrasound as a Tool to Apply Physical Load to Scaffolds and Bone Cells for Fracture Repair

Scott Frazee
UConn, scott.frazee@engr.uconn.edu

Characterization and Implementation of Low Intensity Pulsed Ultrasound as a Tool to Apply Physical Load to Scaffolds and Bone Cells for Fracture Repair

Scott Andrew Frazee

B.S. University of Massachusetts Amherst, 2009

A Thesis

Submitted in Partial Fulfillment of the

Requirements for the Degree of

Master of Science

at the

University of Connecticut

2011

APPROVAL PAGE

Master of Science Thesis

Characterization and Implementation of Low Intensity Pulsed Ultrasound as a Tool to Apply Physical Load to Scaffolds and Bone Cells for Fracture Repair

Presented by

Scott Andrew Frazee, B.S.

Major Advisor _____

Yusuf Khan

Associate Advisor _____

Mei Wei

Associate Advisor _____

Bryan D. Huey

University of Connecticut

2011

Acknowledgements

I would like to first and foremost thank my advisor Dr. Yusuf Khan for his guidance, encouragement, and insight. I would also like to thank my group members: Dr. Kevin Low, Keshia Ashe, James Veronick, Clarke Nelson, Duron Lee, and Farzana Sharmin. They have made this an interesting and enjoyable journey. I would also like to thank the larger Institute for Regenerative Engineering group, especially, Dr. Bret Ulery, and Sean Peach for their insight and valuable help.

I would like to thank my collaborators in Storrs: Dr. Bryan Huey and Vincent Palumbo who provided the fluorescent microscope facilities, as well as guidance with its use and associated software. Without their assistance this work would not have been possible. In addition, I would like to thank Dr. David Knecht and Renee Gilberti who provided the GFP-actin macrophage cells.

Lastly, I would like to thank my family for their love and support in pursuing my dreams, wherever they take me.

Table of Contents

Table of Figures

Abstract

One current challenge in treating bone fractures is the effective treatment of non-unions and delayed unions. Low Intensity Pulsed Ultrasound (LIPUS) has been approved by the FDA to treat fresh fractures since 1994 and non-unions since 2000 and is an attractive treatment option because it is non-invasive. The mechanism by which it works, however, is not well understood; what is known is largely confined to the resultant changes in chemical output of cells. In this thesis several concepts and techniques were brought together to investigate the following hypothesis: LIPUS produces a measurable physical load that results in measurable deformation and displacement of cells and the extracellular matrix (ECM). It is further hypothesized that changing the LIPUS output parameters will result in measureable changes to loading and deformation. This hypothesis was investigated by building and characterizing a variable output LIPUS system capable of applying a load to a GFP-actin labeled macrophage and a self-assembling peptide hydrogel to model the ECM. Loading and deformation were visualized using 3D fluorescent deconvolution microscopy. Analysis of the deformation showed the matrix to have viscoelastic or elastic behavior when compressed, with higher beam intensities showing higher deformations. Cell studies showed physical displacement and increased macrophage fluorescence suggesting heightened actin polymerization in response to loading. These studies describe potentially powerful techniques for investigating the role of other LIPUS parameters in controlling cell and scaffold displacement and deformation.

Chapter 1: Introduction to Bone & Bone Repair

1.1 Physiology

The skeletal system is an important organ system in the body. It fulfills both physiological (hematopoiesis[1] and mineral storage[2]) and mechanical functions (protection of internal organs and locomotion support structure)[1]. The skeletal system contains a significant mineral component (99% of the human body's calcium is found in bone[2]) and acts as a reserve for these physiologically important minerals as well as being important to maintaining the mechanical properties of bone[1]. These functions are of systemic physiological importance; however, they are largely independent of local mechanical properties of bones. In contrast, local mechanical properties can be critical to the mechanical functions of the skeletal system, such as walking, protecting the vital organs, and keeping the brain safe from physical harm.

1.2 Bone Classification

Bones in the body fall into the following classifications based on their geometry: long bones, short bones, flat bones, and irregular bones. In addition, these classifications generally reflect differences in cellular/tissue structure and function. Long bones have one dimension that is dramatically larger than the other two; they are also important in performing gross locomotion (e.g. walking and moving arms)[1]. Short bones are roughly cubic; they are common in the hands and feet[1]. Flat bones have one dimension that is significantly less than

[1] Hematopoiesis is the generation of red blood cells (largely in the bone marrow of long bones). [1]
[2] Ions such as calcium and potassium are important to proper cell function [28].

the other two[1]. Irregular bones are any bone that does not fit into any of the previous categories; the pelvic bone is a prime example[1]. Below, Figure 1, is a diagram of a generic long bone, showing both cancellous and cortical bone, along with medullary (or marrow) canal and the vascular supply.

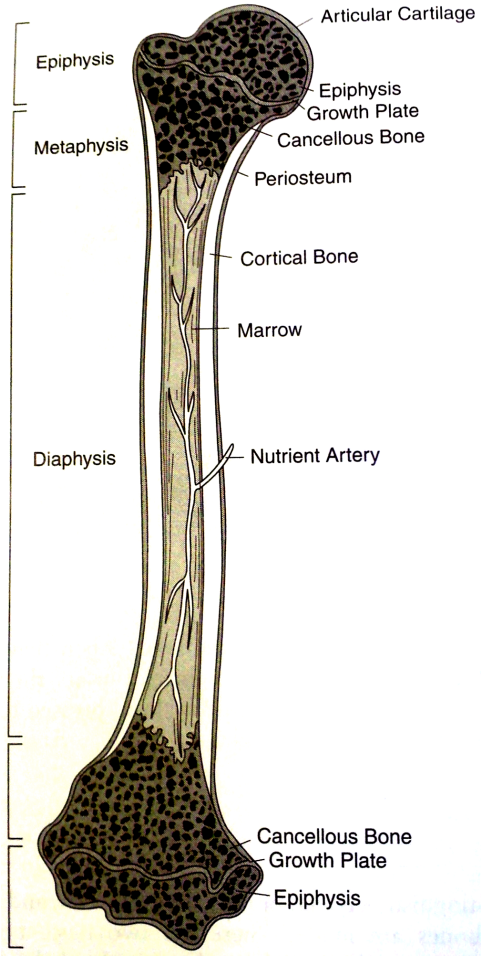

Figure 1: Diagram of generic long bone. Includes cancellous bone, cortical bone, marrow, and vascular supply. (Bartel 2006)

1.3 Bone Tissue

Bone tissue is a composite that consists of several mineral components (mostly hydroxyapatite, a calcium phosphate) and an organic matrix (which is approximately 90% collagen)[2]. On the tissue level the two types of bone are

cortical and cancellous [1]. Cortical bone is also known as compact bone, and is highly dense and composed of many layers or lamellae[1]. Cancellous bone is also known as trabecular or spongy bone and is highly porous network of trabeculae[1]. Cortical bone is several orders of magnitude stronger than cancellous bone[1]. The mechanical properties of cortical and trabecular bone are summarized in the Table 1 below.

Table 1: Mechanical Properties of Human Femoral Bone. Adapted from Athanasiau 2000

		Cortical	Trabecular
Compression	Young's Modulus	4.9-14.5 GPa	123-1600 MPa
	Strength	90-167 MPa	0.15-13.7 MPa
Tension	Young's Modulus	3.9-17.3 GPa	483 MPa
	Strength	90.6-151 MPa	2.5±1.18 MPa

1.4 Bone Cells

There are three types of cells in bone: osteoblasts, osteoclasts, and osteocytes [3]. Osteoblasts have two main roles: bone matrix[3] formation and regulation of osteoclasts [3]. Osteoclasts are giant cells that are responsible for resorption of ossified bone tissue. Giant cells in general and osteoclasts specifically are formed from the fusion of several cells and are approximately 20-100 microns in diameter and have a high concentration of lysosome vesicles which are essential

3 bone matrix: flexible protein matrix in which minerals such as calcium and phosphorus are deposited and form bones. <Mosby's Dictionary of Complementary and Alternative Medicine. (c) 2005, Elsevier>

to their bone degradation function [3]. Osteocytes are osteoblasts that have become embedded in the bone matrix; this results in morphological and biochemical changes [3]. These cells form a syncytium[4] similar in structure to a neural network; it is broadly theorized that they play a role in monitoring mechanical conditions experienced by bone[3]. Both osteoblasts and osteocytes have been shown to be sensitive to shear stress in vitro, producing responses associated with mechanical loading of bone in vivo; such as decreased apoptosis and changes in NO and PGE2 production[4].

1.5 Fracture Repair

In order to understand interventions in fracture healing, a brief synopsis of the normal healing processes is warranted. Fracture healing is a natural process that occurs after bone fracture occurs. It follows a specific set of phases or steps that result in the healed bone being largely indistinguishable from pre-fracture bone. Browne identifies five stages of normal fracture healing in cortical bone, illustrated schematically below in the Figure 2. The stages are: (I) Clot formation, (II) Capillary invasion, (III) Collar formation, (IV) Clinical Union, (V) Consolidation.

[4] syncytium: a group of cells in which the cytoplasm of one cell is continuous with that of adjoining cells, resulting in a multinucleate unit <Mosby's Medical Dictionary, 8th edition. © 2009, Elsevier.>

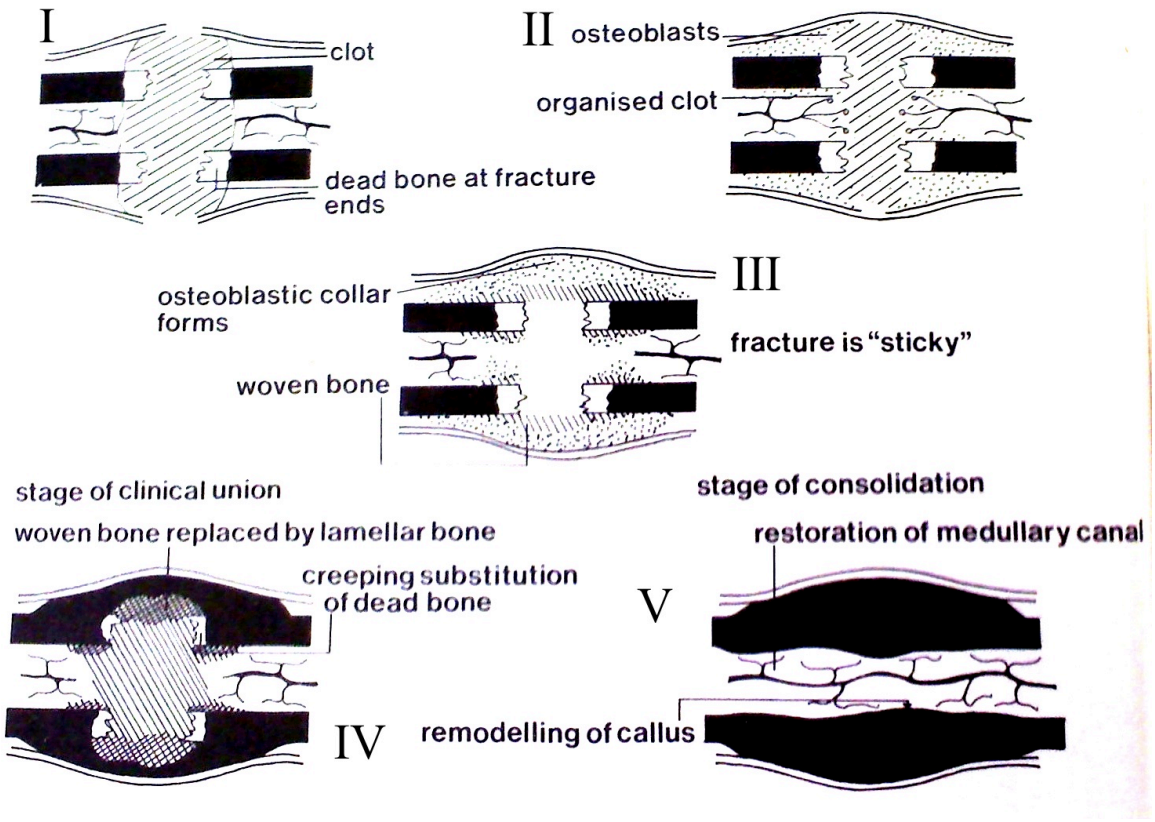

Figure 2: Schematic of the stages of healing in cortical bone. At Stage I, clot formation has occurred; at Stage II, revascularization of the fracture has begun; at Stage III, a semi-rigid osteoblastic collar has formed, creating a 'sticky' fracture; at Stage IV, lamellar bone has replaced the osteoblastic collar uniting the fracture, achieving 'clinical union'; at Stage V, the medullary canal has been fully restored and remodeling progresses to remove signs of the fracture. Adapted (Browne 1983)

During the first stage bleeding occurs due to damage to the bone and soft tissue, with subsequent clot formation; cell death also occurs due to loss of vascular supply[5]. During the second stage capillaries invade the clot and create granulation tissue[5]; osteoblasts also begin to proliferate in the granulation tissue[5]. During the third stage an osteoblastic collar is raised at the bone edges

[5] granulation tissue: the newly formed vascular tissue normally produced in healing wounds of soft tissue, ultimately forming the cicatrix. Dorland's Medical Dictionary for Health Consumers. © 2007 by Saunders

and forms woven bone that bridges the bone gap; this occurs around three weeks after fracture[5]. The collar stabilizes the fracture, though it remains partially mobile[5]. During the fourth stage the woven bone is transformed into dense lamellar bone; once no detectable movement occurs the fracture is deemed 'clinically united'[5]. During the fifth stage the medullary cavity[6] is restored and excess bone is removed during remodeling[5].

Some fractures, however, do not follow this normal healing process. For example, a simple tibia fracture should heal to clinical union after 13 weeks; however, if this has not occurred after 18 weeks it is considered a delayed union[5]. Non-unions are an ever more extreme form of abnormally healing fractures that will never heal on their own without the addition of some supplementary treatment[5]. Both delayed unions and non-unions are candidates for treatment with bone grafts[5]. Cancellous bone undergoes a similar healing process, but has a much richer blood supply and does not usually result in non-unions[5].

1.5.1 Fixation Methods

Fracture healing is an important focus of modern orthopedics. Orthopaedic options for fracture healing broadly consist of two categories: fracture fixation and bone grafts. Such methods facilitate the natural healing processes. Fixation may come in a very limited form such as casts, splints, and traction; these methods do

[6] medullary cavity: the marrow cavity in the shaft of a long bone. American Heritage® Medical Dictionary Copyright © 2007, 2004 by Houghton Mifflin Company

not hold the fracture completely rigid and allow some movement[1]. Other surgical approaches hold the fracture more rigidly in place; such methods include screws, plates and intramedullary rods[1]. Their main function is to provide mechanical support and (partial) isolation of the fracture site to allow relatively normal motion while the body heals the fracture on its own[5]. The fixation also maintains proper alignment of the bone fragments so they heal straight[1].

1.5.2 Bone Grafts

Occasionally the body is unable to heal a fracture on its own or a large section of bone needs to be removed and replaced. This is where bone grafts are used. These can be divided into natural grafts (i.e. autografts and allografts) and bone graft substitutes. Currently the gold standard of grafts, in terms of functionality, is the autograft. An autograft is a section of bone harvested from the patient's own body (usually the iliac crest) and implanted elsewhere in the body. The main advantages of using autografts is the lack of disease transmission risk, excellent integration due to lack of rejection and the presence of osteoinductive[7] biological elements, such as live bone cells and growth factors. The major disadvantages include donor site morbidity[8], and limited supply (including quantity, size, and type of bone).

[7] osteoinductive: capable of stimulating the development and formation of bone tissue

[8] Donor site morbidity is any disease or abnormal condition at the site or location in the body where bone (in this case) was harvested. Graft site morbidity is also possible. Possible conditions include bleeding, pain, and necrosis.

Allografts are similar to autografts in that they are harvested from the body; however, in this case they come from another patient or a cadaver. This introduces the risk of disease transmission and necessitates sterilization of the graft, which destroys the active biological components that aid in the integration of autografts. The advantages which allografts bring include fewer (though still present) limitations on supply, and in the case of cadaver sources, a wider selection of bone type, shape, and size, and no donor site morbidity.

Bone graft substitutes represent an important and growing alternative to autografts and allografts, given their shortcomings. Research in bone graft substitutes seeks to achieve the success of autografts without their considerable limitations. One major advantage of bone graft substitutes is that they are manufactured and therefore do not face the supply limitations of natural grafts.

One of the current challenges in orthopedics in the area of fracture healing is reliable treatment of non-unions. Often these are treated by a combination of growth factors and bone graft substitutes. Sometimes, however, alternative less invasive treatment methods such as ultrasound are used to induce fracture repair. Ultrasound in particular is attractive because it is non-invasive.

Chapter 2: Introduction to Ultrasound

2.1 Theory of Sound

To understand the mechanical interactions of ultrasound in bone repair, a basic definition of sound and review of acoustics[9] is in order. Modern (linear)[10] acoustics emerged as a coherent theory in the 19th Century, mainly through the contributions and consolidations of Lord Rayleigh, especially his 1877/1878 work "The Theory of Sound"[6-8]. Ultrasound, as a distinct field of interest, came to prominence during WWI for its use in underwater acoustics in submarine detection[6].

David Blackstock provides an excellent description of sound in his book Fundamentals of Physical Acoustics. Sound, he points out, is a particular kind of wave, and for the purpose of this thesis, Blackstock's summary description of a wave will do:

> *A wave is the movement of a disturbance or piece of information from one point to another in a medium (except that electromagnetic waves do not require a medium). The movement takes place at finite speed. The disturbance moves with respect to the medium. The shape or form of the disturbance is arbitrary.*

[9] Acoustics: The scientific study of sound, especially of its generation, transmission, and reception. The American Heritage® Medical Dictionary Copyright © 2007, 2004

[10] Sound is generally considered to behave linearly (i.e. exhibit the same properties / behavior regardless of scale such as signal amplitude); this generally works, however, at extremely large amplitudes this assumption noticeably breaks down, such as in sonic booms, where the speed of sound is not constant for all wave amplitudes. The boom is a large discontinuity in pressure that results from the non-uniformity of the 'speed of sound' (i.e. the rate or speed of signal propagation).

Sound can then be more narrowly defined as a mechanical compression wave (i.e. a wave in a physical medium where the disturbance involves the compression and rarefaction of the medium). It should also be noted that no part of the definition mentions frequency or oscillation. While these are often important components of a wave, they are not necessary. That not withstanding, sound is often assumed to be composed of (superimposed) sine waves to simplify modeling. Given that a sufficient summation of sine waves can create any arbitrary shape, this is not entirely inaccurate, though it may be misleading due to oversimplification.

It should also be noted that in general a disturbance can have two possible relations to the direction of propagation: perpendicular or parallel. In a transverse wave the disturbance moves perpendicular to the direction of propagation; electromagnetic waves are a prime example. Alternatively, in longitudinal waves, the disturbances moves parallel to the direction of propagation; sound waves are of this type. Longitudinal and transverse waves are illustrated schematically in the Figure 3.

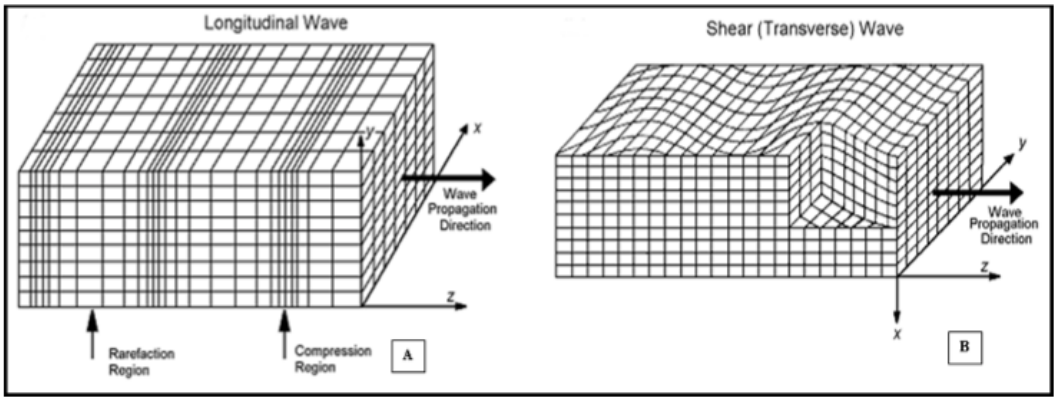

Figure 3: Longitudinal (A) and Transverse Wave (B). In the Longitudinal wave, the signal or waveform is represented by areas of rarefaction and compression of the media (as is the case with sound). In the Shear wave, the signal or waveform is represented by movement perpendicular to the direction of wave propagation (as is the case with light or vibrating strings in musical instruments). (Cobbold 2007)

2.1.1 Properties of Fluid Media in the Context of Acoustics

Fluids are often treated as continuous media for analytical purposes and this agrees well with intuition and everyday experience. However, all matter is composed of discrete units of atoms or molecules, which are not the same as the fluid particles seen in the Figure 3 (i.e. the cubes). In the context of acoustics and fluid mechanics, a fluid particle is a volume of fluid, such that the average motion of all the molecules of the fluid is zero (note: fluid particle vs. molecule of the fluid).

Similarly, fluid velocity refers to the velocity of a fluid particle (and thus net fluid movement) rather than the velocity of an individual molecule (which may have a different direction and magnitude than the fluid particle in which it is contained). One important reason for defining a fluid particle is to be able to describe fluid

velocity, which may not be spatially or temporally uniform, independently from molecular motion; similarly, other macroscopic properties (e.g. pressure, temperature, entropy) may be tracked by fluid particle. These properties can be important to acoustics, specifically the amplitude of a sound wave, which is the deviation of the pressure of a fluid particle from its average undisturbed pressure. Blackstock describes the following thought (or gedanken) experiment to illustrate the concept of a fluid particle:

> [C]onsider a *gedanken* experiment in which the density [**ρ**] of a gas at rest is measured. Weigh a box of gas, subtract the weight of the box, and divide by *g* to get the mass *M* of the gas. Finally, divide *M* by the box volume *V* to obtain the density. Now cut the box in half and repeat the measurement. The density is of course the same: half the volume of gas has half the mass. Repeated halving of the box are found to have no effect on density — up to a point.

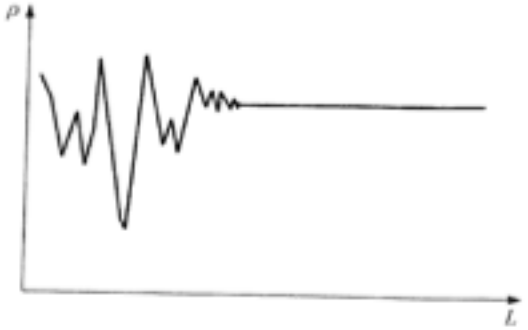

Figure 4: Dependence of the measured density (ρ) of the gedanken box/fluid particle on the characteristic length (L) of the box/particle. This shows why a fluid particle has to have a minimum set of dimensions for it to be able to represent the local density (or other bulk property) for a section of fluid. In other words, a fluid particle has a minimum size that it can be reduced to before noise fluctuations mask the local changes in the bulk properties that makes a fluid particle a useful concept. Once you get all the way down to the scale of an atom or molecule you are seeing thermodynamic statistical distributions rather than fluid speed or density. (Blackstock 2000)

Blackstock further points out, the probability of evenly dividing the molecules decreases as the size of the box decreases, causing the density measurements to become increasingly erratic as Figure 4 shows. Thus, the notion of the density of a fluid particle makes sense, given a large enough particle volume. Other macroscale properties such as pressure, temperature, and fluid velocity are similarly tied. These properties are important to understanding how ultrasound interacts with the body, and thus an understanding of what is measured is similarly important. Understanding fluid media is particularly pertinent because the body is largely composed of water, thus the major medium through which ultrasound travels when used clinically. Water is also the medium through which ultrasound travels in the visualization experiments performed in this thesis.

2.2 Medical Ultrasound

The “ultra” prefix in ultrasound denotes a frequency above 20 kHz (i.e. above the frequency range that the human ear can hear). There is a correspondingly labeled “infra” sound that is at a frequency below human hearing. There are several medical applications of ultrasound. For example high intensity focused ultrasound has been used for tissue ablation as an alternative to invasive surgery, most frequently for ablating cancerous tumors[6]. High intensity focused ultrasound works to ablate tumors by causing localized heating which cause cell death or extreme vibrations which shake the cells apart causing lyses[6]. Since the mid 1990s the FDA has approved Low Intensity Pulsed UltraSound (LIPUS)

devices for therapeutic applications, specifically for treating fresh fractures in 1994 and nonunion fractures in 2000[9]. LIPUS, as the acronym implies, is a specific subset of ultrasound, which is of low intensity (amplitude) and which is pulsed (at regular intervals) rather than applied as a continuous wave. In clinical applications, LIPUS is typically administered according to the following parameters: 20-minute daily treatment, 1 MHz or 1.5 MHz carrier wave, 1kHz pulse rate frequency, 20% duty cycle, and an average intensity of 30 mW/cm^2[9]. To begin to understand the physical interaction of LIPUS with osteoblasts it is important to understand what LIPUS is, as a physical phenomenon. This is important, as there are several aspects of ultrasound, which are often under-appreciated from the cellular biology perspective.

2.2.1 Ultrasound for Bone Repair

In contrast to High Intensity Focused Ultrasound, the mechanisms by which clinical LIPUS works are not well understood[9]. Much of what is known is confined to the changes in cellular signaling that accompany its application as well as the resulting macro-scale bone formation[9]. There is a missing intermediate step that must be understood to maximize the utility of LIPUS. Broadly, the two-part question to be answered is “how does LIPUS physically interact with cells and what, if any, part of this interaction is important to osteogenesis?” The focus here will be on the broader first part of the question. One theory put forth by the work described herein is based on the possibility that

ultrasound stimulates the well-studied reaction of bone to physical loading, a theory described by Wolff's Law.

Chapter 3: Literature Review

3.1 Wolff's Law

As mentioned previously bone is constantly being remodeled on a cellular level. This remodeling produces a geometry that most efficiently carries the stress that is applied to the bone. Julius Wolff observed in his 1892 publication Das Gesetz der Transformation der Knocken [lit.: Laws of Bone Transformation]: "Every change in the form and function of bone or of their function alone is followed by certain definite changes in their internal architecture, and equally definite alteration in their external conformation, in accordance with mathematical laws." (1986 Springer-Verlag translation quoted in H. Frost 1994)[10] This observation is known as Wolff's Law. The law can be summarized with the following statement: "bone is deposited and resorbed in accordance with the stresses placed upon it."[3].

More recent studies have sought to find the mechanisms though which Wolff's Law acts[11]. There are two mechanostats that regulate bone strength, through the control of bone resorption and bone deposition; these mechanostats act similarly to a pair of thermostats controlling the temperature of a room, through negative feedback loops[11]. One of the broadly accepted gauges of bone stress is shear stress felt by osteocytes. Fluid flow is produced in lacunae–canaliculi channels occupied by osteocytes by pressure gradients produced during

mechanical loading of bones and their subsequent deformation[12][13]. Such sensitivity to fluid flow is an example of mechanotransduction.

3.2 Mechanotransduction

Broadly, cellular mechanotransduction is the conversion of mechanical forces "into chemical signals inside the cell ... [which] elicit a cascade of cellular and molecular events"[14]. There are several pathways by which mechanotransduction is achieved[13]. In bone the mechanotransduction mechanisms are believed to be mechanosensitive ion channels and integrin adhesions[13]. What is more controversial is what the primary mechanical interaction which triggers these mechanisms, specifically whether it is shear flow, shear drag, or membrane strain[13]. The dense rigid mineralized matrix of bone shields the cells from compressive forces, and inhibits direct sensation of such forces; physiological strain induced in bone is approximately .04%-.3% which is orders of magnitudes lower than strains observed in vitro to produce cellular responses (1%-10%)[14][15]. More recent work has suggested that strain is the dominate mechanisms of mechanotransduction in osteocytes; specifically shear drag on the matrix is approximately 20 times greater on the ECM than cell surface, this results in an even greater cell strain caused by matrix deformation rather than directly through fluid forces on the cell[13]. By extension, osteoblasts in a deformable matrix may be similarly stimulated. This notion may help guide

the development of new treatment modalities through the design of novel scaffolds for bone repair and regeneration.

3.3 LIPUS & Osteoblasts

Some studies show that dynamic loading of bone produces inter-canalicular flow, subjecting bone cells to shear flow; the effects of force versus shear flow in vivo may be inseparable[13][16]. Osteoblasts respond initially at the onset of steady shear flow but the response diminishes over time[12][13]. These studies were followed with pulsatile shear flow experiments that demonstrated a more sustained response than steady shear flow[13].

In parallel, there have been studies on the response of osteoblasts to ultrasound and LIPUS, which have shown similar cellular responses[9][17]. These results suggest that LIPUS may be producing a shear flow (at least in vitro), which may be responsible for the observed clinical results. In addition, other studies have shown that US is capable of producing unidirectional flow as well as non-zero time average unidirectional force[18][19-21][22][23]. This is another potential mechanism by which LIPUS produces clinical results. The specific mechanism(s) by which ultrasound interacts with cells, however, largely remains an open question.

3.4 Sound as Force

There are two interesting non-zero time average quantities that arise from LIPUS. The time average velocity and the time average pressure. The former is referred

to as acoustic streaming. The latter is referred to as acoustic pressure or the acoustic radiation force. The radiation force was first measured in 1903[24]. Measuring this force is a common method for quantifying the output of clinical ultrasound[25][26]. Torr showed that the observed force is the result of “the transfer of wave momentum.”[24] The force may then be translated into energy flux or beam intensity. Ultrasound beams in fluid media have also been shown to be accompanied by acoustic streaming (i.e. fluid flow in or surrounding the beam and generally moving in the direction of beam propagation)[6].

Sound in general, and ultrasound specifically, has been well established as capable of producing fluid flow in media and physical force in absorbing targets. Observations of fluid flow date back to at least Lord Rayleigh’s observation of so called Quartz Winds[7]Later Eckart explored the ability of acoustic beams to produce accompanying streams of fluid flow. Sound waves, similarly to other types of waves (e.g. electromagnetic) are known to apply a force to absorbing targets[18]. Torr elucidated the theoretical basis for this in sound beams[24]. Measuring the physical force produced by ultrasound equipment is the standard output calibration technique for FDA approved medical devices (both therapeutic and diagnostic).

3.5 Tying It All Together

There are several diverse concepts that are united in this thesis and are beginning to be united in the general research community. The foundational

ideas are well established: ultrasound has been used to produce force and fluid flow, ultrasound is used clinically to induce fracture repair; force is well established in shaping bone on a tissue level, bone cells respond with an up regulation of various key markers in response to physical force/shear stress.

Other sources have suggested that ultrasound exerts a physical force/deformation on bone cells that is important to accelerating fracture repair. However, to the author's knowledge, this has never been directly observed. This thesis proposes to demonstrate that clinically relevant ultrasound does produce an observable physical force, which is able to deform and displace osteoblasts and ECM, suggesting an explanation for that missing link in understanding the mechanisms by which clinical LIPUS works.

3.6 Research Objectives

The hypothesis of this study is that Low Intensity Pulsed Ultrasound is capable of producing a measurable physical load; it is further hypothesized that LIPUS can be used to apply a load to cells and scaffolds to produce measurable deformation and/or displacement, which may be useful in bone fracture repair. The work described below has been organized into 3 specific aims:

Specific Aim 1: To design and characterize a LIPUS system with tunable output parameters that will enable variable control over LIPUS signal

variables. It is hypothesized that a highly tunable LIPUS system will result in a measurable physical load that can vary with modified input parameters. Signal amplitude, frequency, duty cycle, and distance from transducer to target will be varied. Ambient heating will be evaluated to ensure that chosen LIPUS intensities do not result in excessive and potentially harmful local heating.

Specific Aim 2: To visualize and quantify the physical loading and deformation of a scaffold using the LIPUS system designed in Specific Aim 1. It is hypothesized that a tunable LIPUS system will result in distinct loading and deformation of the scaffold that vary with modified LIPUS parameters. Signal amplitude and duty cycle will be varied.

Specific Aim 3: To visualize the physical loading, deformation, and displacement of a cell using the LIPUS system designed in Specific Aim 1. It is hypothesized that a tunable LIPUS system will result in distinct displacement and/or deformation of the cell that varies with modified LIPUS parameters. Signal amplitude and duty cycle will be varied.

Chapter 4: Materials & Methods

The LIPUS system was designed to give a high degree of control and verification over the output parameters; this level of control is not available from commercially available clinical devices currently used to treat fractures and fracture non-unions such as the Exogen unit from Smith & Nephew, which are

widely used for LIPUS experiments described in the literature[12]. Specifically the system is capable of varying the waveform (sinusoidal, square, etc.), signal amplitude, duty cycle, and pulse rate frequency, and carrier wave frequency. Much of this control was achieved by selecting a Function/Arbitrary Waveform Generator, paired with a Broadband Power Amplifier to produce the desired output levels. For ultrasound generation the waveform generator/amplifier was paired with a commercially available immersion transducer

4.1 Specific Aim 1: Ultrasound Parameter Verification

These preliminary studies were designed to verify the output parameters of the equipment and their relevance to clinical work. The waveform was generated by an Agilent 33210A 10MHz Function / Arbitrary Waveform Generator. The signal was verified on a GwInstek GDS-1102A Digital Storage Oscilloscope (100MHz 1G Sa/s). The signal was amplified on an ENI 403LA Broadband Power Amplifier (37dB, .15-300MHz, 1V Max) before being sent to the 1MHz transducer, which was purchased from Olympus-IMS. The temperature rise was measured with an OakTon Acorn Series Temp JKT Thermocouple (P/N 54X243542). The force was measured with a Mettler Toledo Classic Plus <AB104-S/FACT> digital scale in conjunction with an absorbing target in a sound-absorbing container.

4.1.1 Heating Measurements

While the exact mechanism behind the utility of LIPUS as a treatment for fracture repair is unknown, one theory suggests that the ultrasound raises the local temperature of the tissue and enhances healing through this mechanism. While

minor local temperature increases may not be harmful, higher intensity ultrasound can raise local temperatures considerably (see section 2.2 on Medical Ultrasound). Given these two scenarios, local temperature was monitored to answer two questions: 1) does LIPUS raise local temperatures to a degree that may be harmful to cells for in vitro experiments and 2) can local heating be responsible for any effects seen during testing.

The FDA mandates that local temperatures for LIPUS treatment not increase by more than 1ºC. For that reason temperature measurements were made to determine temperature rise due to ultrasound. The measurements were taken in a 37ºC warm room, using the following set up, depicted in the Figure 5. The setup consisted of BD 6-well plates <Cat # 351146> filled with DI water. The water was allowed to equilibrate to 37 °C overnight. The ultrasound transducer was then placed into a well and run with the specified parameters for 20 minutes. The temperature of the water was measured at the start of each run, and then at 5-minute intervals. The study was performed with an n of three and mean values were determined.

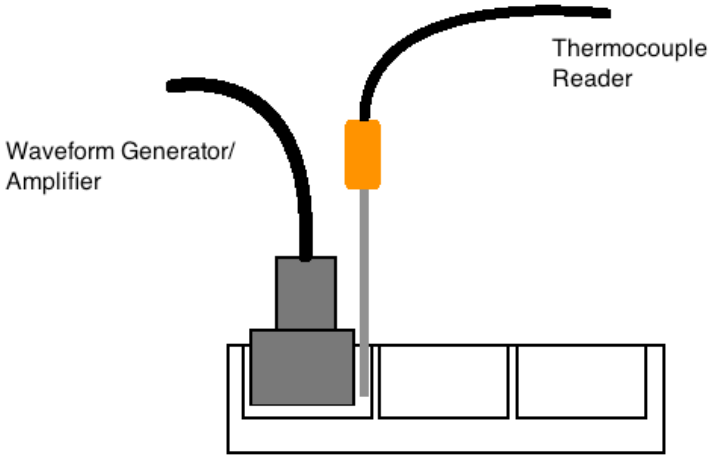

Figure 5: Schematic of Ultrasonic Heating Experimental Set-Up, with well plate, transducer and thermocouple. The 6-well plate (each well filled with DI H_2O), immersion transducer, and thermocouple were left in a 37 °C warm room overnight in order to reach equilibrium temperature. The immersion transducer was then placed in a well and run with specified parameters for 20 minutes. Temperature of the water was measured at the beginning of US exposure and then at 5-minute intervals for the duration of exposure. This processes was repeated for each set of US output parameters in a different well.

4.1.2 Force Measurements

The purpose of the force measurement study is two fold: 1) to verify that the system is capable of producing a controlled measurable force (i.e. it works and one can tell what force is being produced), and 2) to be able to compare the effects in Aims 2 and 3 with each other and other studies using beam intensity (which can be determined from measuring the force the beam applies to an absorbing target and knowing the cross sectional area of the beam). The force was measured on a Mettler Toledo digital scale. The force was transmitted though a wire attached to an absorbing cone that absorbed the ultrasound beam transmitted by the Olympus transducer. The signal was generated as specified

by the previous section. The set up is shown below in Figure 6. In essence, the transducer was immersed in the water and pointed at the cone, which was suspended by a pair of wires attached to a weigh hook on the bottom of the digital scale. The transducer produced an ultrasonic beam, which propagated through the water in the container and was absorbed by the cone. This absorption resulted in momentum transfer from the water to cone, essentially applying a force to the cone in the direction of propagation of the ultrasound beam. The cone then transmitted that force to the weigh hook on the scale through the aforementioned wires. The scale then measured the force on the weigh hook.

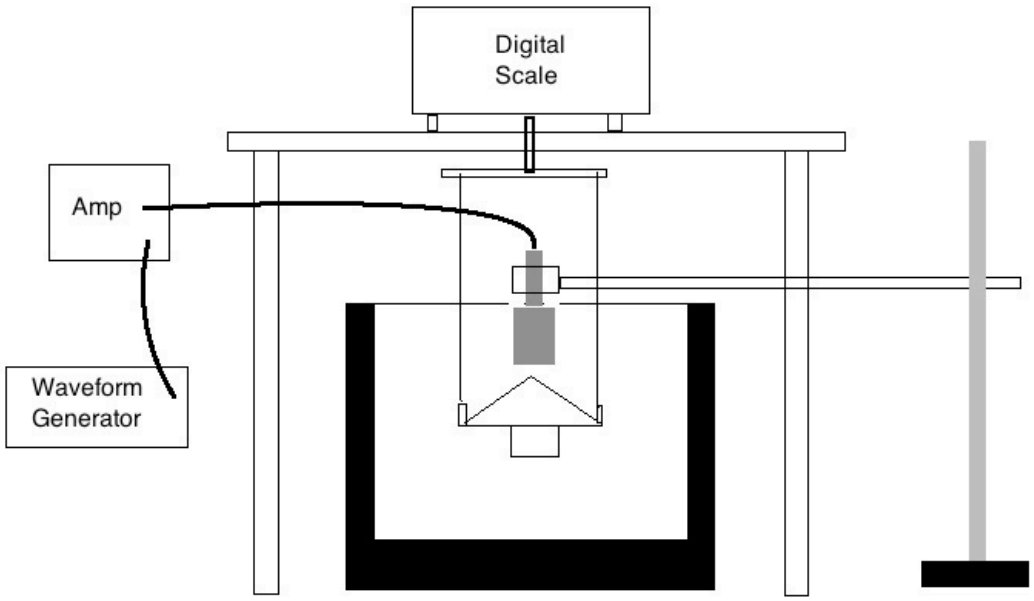

Figure 6: LIPUS force measurement setup, including Waveform Generator, Amplifier, Immersion Transducer, Digital Scale, and Absorbing cone. The transducer is partially immersed in water and is held in place above and pointed down at the absorbing cone. The transducer is held in place by an attachment to a ring stand. The absorbing cone is suspended in the DI H_2O by a pair of wires, which are attached to a weigh hook at the bottom of the digital scale. The beam produced by the transducer

is absorbed by the cone, which applies a force to the cone. The cone then transmits the force to the weigh hook through the wires by which it is suspended. The digital scale then measures the force on the weigh hook.

The experiment was performed with an n of 3 or 4 (depending of the beam parameters). Mean values were determined. Beam power, beam intensity and relative output compare to 500mV continuous wave 1MHz carrier wave for the beam parameters used in Specific Aims 2 and 3 were calculated.

4.2 Specific Aim 2: Mechanical Interaction with Scaffold

4.2.1 Beads in PuraMatrix

A commercially available peptide hydrogel (BD PuraMatrix) was used as a synthetic ECM and was reconstituted according to manufacturer's instructions. PuraMatrix (PM) is a 3-D peptide hydrogel that self-assembles to mimic the mechanical and topographical qualities of natural ECM when exposed to a salt solution. It is marketed to provide a 3D environment for culturing cells, especially those that naturally grow in a 3D environment and do not culture well on standard 2D tissue culture plastic. Both the fiber strands (7-10nm diameter PM vs 5-10nm diameter ECM) and the porosity (50-200nm PM vs 50-400nm ECM) are very close to natural ECM[29]. These and other properties are compared for PuraMatrix, ECM, and other ECM substitutes in Table 2 below.

Table 2: Comparison of the key characteristics of PuraMatrix with natural ECM and other ECM substitues. Taken from (PuraMatrix Comparsion & Characteristics)

Characteristics	PuraMatrix™ Synthetic ECM	Natural ECM	Synthetic Scaffold	PuraMatrix™ Advantages
Composition	Patented 16 mer peptide in 0.5-1.0% w/v	Collagen, Fibronectin, Cadaver tissue, Basement membranes	PLA, PLGA, carbon fiber, calcium phosphate	Animal-free, reproducible cell culture & cell signaling.
Fiber Size:	7 – 10nm Diameter	5 – 10 nm Diameter	10,000 – 100,000 nm Looks 2D relative to cell	Approximates in vivo ECM nano-scale
Pore Size:	50 – 200 nm	50 – 400 nm	20,000 – $1x10^6$nm	Encapsulates like ECM
Water Content:	99.5 – 99.9%	80 – 97%	60 – 80%	Better hydration & nutrient diffusion
Mechanical Strength	Low to mid, cells can migrate within it	Low to mid	Mid to High	More rapid ingrowth, breakdown

Briefly, the hydrogel stock solution (1% w/v) was sonicated for 30 minutes and pipetted into a culture well plate. The solution was then pipetted onto a glass cover slip, mixed with salt solution and allowed to gel for 30 minutes at room temperature. The salt solution was replenished twice over 60 minutes.

To visualize the movement of the matrix under LIPUS stimulation, 10 μl of a fluorescent 1-μm diameter polystyrene bead suspension (Fisher Scientific, Inc.) was pipetted into each well prior to gelation. There are several advantages to this approach. The 1-μm diameter beads were selected under the assumption that they would track the motion of a fiber in which they were imbedded better than a larger bead, which would be more likely to sit between fibers. Furthermore, the goal was to track the movement of the gel caused by the ultrasound, and it was believed that with a smaller bead would absorb less of the ultrasound (at least by virtue of having a smaller cross-sectional area). Thus a smaller bead would be less likely to change the movement of the gel, and would better represent the movement of the gel that would occur without any beads present.

Hydrogels were exposed to ultrasound with a carrier frequency of 1MHz and amplitudes of 200mV and 500mV (peak to peak), pulsed at 1kHz. The duty cycle was set variously to 20%, 50% and 100% (i.e. continuous wave). Imaging of beads within the hydrogel was performed using a Nikon optical microscope equipped with epifluorescence, and a water-cooled digital camera (Hammamatsu, Inc.). Images were collected and evaluated using Volocity Software, (Improvision, Inc.). Additional image preparation was performed using ImageJ and SketchBook Express. Individual punctate light sources (either a single bead or a small group of beads) were tracked. Displacements were evaluated qualitatively based on bead diameters travelled. Comparisons were made based on applied force / relative beam intensity (based on calculations from Aim 1).

4.3 Specific Aim 3: Mechanical Interaction with Cell

4.3.1 GFP-actin Macrophages on Glass

GFP[11]-actin expressing cells were chosen for cell deformation imaging for two main reasons: 1) the many practical advantages of not needing to stain the cells, and 2) the ability of the GFP-actin to indicate cytoskeletal rearrangement in the

[11] GFP stands for Green Fluorescent Protein

cell. Specifically, F-actin[12] polymerization is visually identifiable in the cells as areas of increased fluorescence[27]. F-actin polymerization is indicative of actin filament formation, which occurs during cytoskeletal rearrangement[28]. Actin filaments are found in high concentrations just below the cell membrane, providing a good visualization of the cell (membrane)[28]. In addition, actin filaments form cellular projections such as lamellipodia and filopodia, which the cell uses to explore and move[28].

Simply put, the GFP-actin macrophages are suitable for visualizing the outline of the cell as well as active cytoskeletal rearrangement. In addition, because the cells express GFP on their own there are no extra complicating steps or dyes involved in cell fluorescence. This eliminates problems such as trying to stain a cell in situ once it is embedded in a hydrogel. Another problem introduced with staining cells is that, there is the distinct possibility that the stain will change both the mechanical properties of the cell (because the stain is embedded in the cell membrane) and the behavior of the cell (because stains are often toxic to cells). The second reason for choosing this particular cell type is that the GFP is linked to actin. The cell has been shown to light up during active cytoskeletal

[12] F-actins, also known as actin filaments, are important cytoskeletal elements which are concentrated below the cell membrane and "determine the shape of the cell's surface and are necessary for whole-cell locomotion"[28].

rearrangement such as in response to engulfing a foreign body or moving in response to an applied stress[27].

The GFP macrophage cells were cultured and treated as described by Palumbo [27]. Briefly, the macrophages were transfected with DNA for expressing Green Fluorescent Protein-bound-actin, and then cultured on #1.5 thickness cover slips. The cover slips were then transferred to the fluorescence microscope. Imaging of the macrophages on the coverslip was performed as described in Specific Aim 2. Cell displacements were evaluated qualitatively based on displacements relative to the size of the cell. The cells were also evaluated qualitatively for actin activity and deformation.

Chapter 5: Results

5.1 Specific Aim 1: Ultrasound Parameter Verification

5.1.1 Heating Measurements

These preliminary studies were done to characterize the output parameters of the ultrasound system. For the heating study, the increase above ambient temperature is summarized in the Figure 7. The study was done to address two concerns: 1) whether the device was producing conditions which would be within FDA guidelines and what the maximum intensity might be while remaining within those conditions, which is important to clinical relevance, and 2) whether any changes in cell behavior can be safely assumed to be independent of heating

effects, as the focus of this study is the mechanical interaction of ultrasound. If heating were found to be minimal or negligible (i.e. less than 1°C), any changes would be considered independent of any residual heating. These heating results are specifically applicable to in vitro studies (rather than in vivo) because the heating measurements were performed in the relatively small volume containable within 6-well plates.

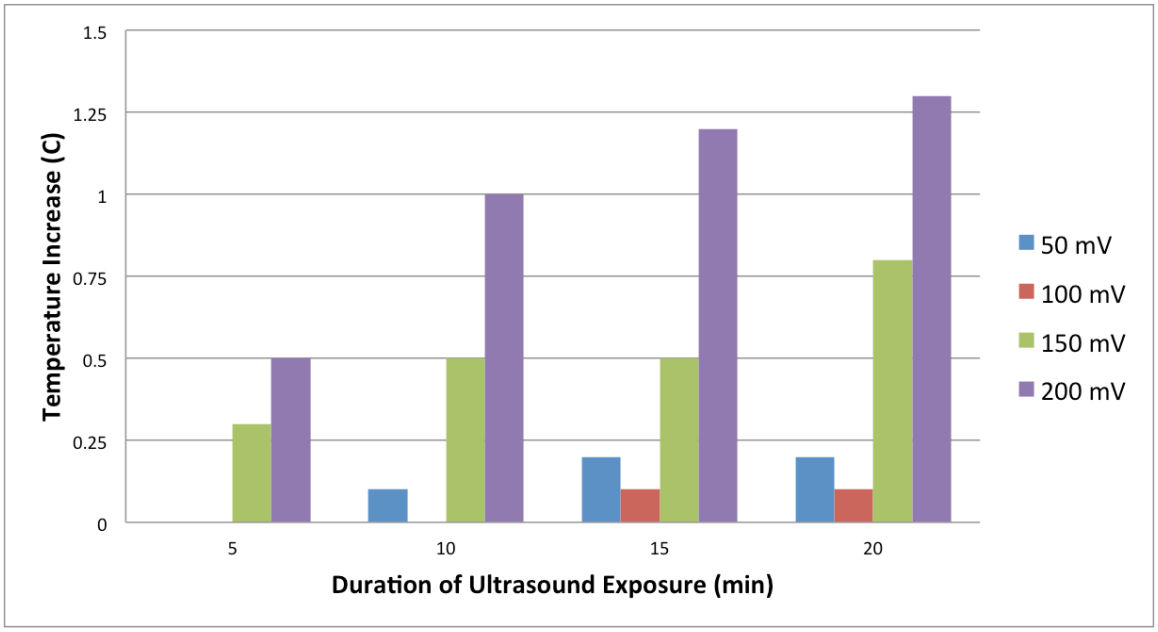

Figure 7: Heating Effects of 1 MHz Pulsed Sine Wave with a 20% duty cycle and 1 kHz pulse rate frequency. For all sets of parameters except 200mV after 15 minutes the temperature rise did not exceed 1 °C, the FDA mandated limit for local heating induced by ultrasound devices. These conditions represent a worst-case scenario that would not be seen in vivo where the body is able to transfer excess heat away through fluid flow. It should also be noted that the most extreme conditions here only barely exceeded 1.25 °C rise after 20 minutes of exposure in a warm room to ultrasound of greater intensity than is currently in use clinically.

As can be seen in Figure 7, heating increased with signal amplitude and exposure time. Only the most extreme conditions caused a temperature rise of

greater than 1°C above ambient: the FDA limit for acceptable temperature rise in ultrasound devices.

5.1.2 Force Measurements

The purpose of the force measurements was to 1) characterize parameters relevant to clinical use (i.e. beam intensity as measured by equivalent force) and 2) be able to tune the output parameter under general investigation in the study, specifically to include intensities used clinically (5-10mg which corresponds to 25.7-51.4 mW/cm^2 intensity at 1.5MHz carrier wave, 1kHz pulse rate frequency for a 1.9 cm (0.75 inch) beam diameter). The force output is well defined, as shown in Figure 8 below. While the output is not exactly linear, such a representation provides a fairly good fit (all R^2 values are greater than .97) with low noise. This means than a desired force can be easily selected by modifying the input voltage. Specifically, force outputs of 5-10mg, which represent a range of 25.7-51.4 mW/cm^2 intensity and are similar to therapeutic LIPUS applications (30mW/cm^2 for fracture repair), are easily achieved for all duty cycles.

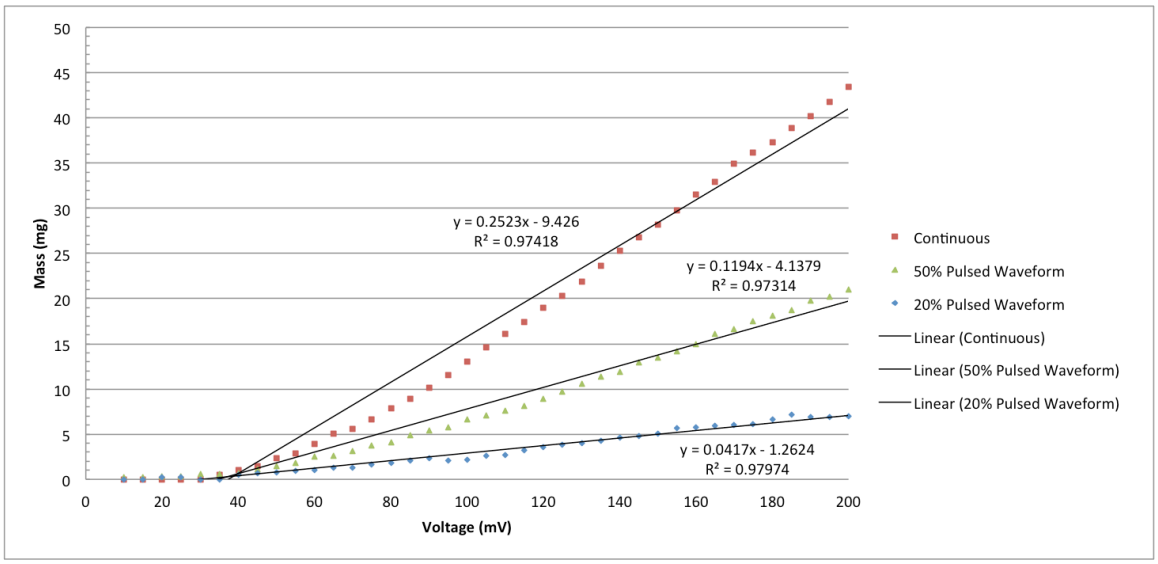

Figure 8: Load Comparison of Pulsed versus Continuous Wave for 1 MHz signal. The Force vs Voltage curves are well defined by the 3rd degree polynomial best-fit lines for each of the duty cycles shown on the graph, with R^2 values above 0.97 for all three. While the lines are not quite linear, they are fairly free of noise. This shows that desired force/beam intensity can easily be selected by changing the voltage for a variety of duty cycles.

The proportional relationship between the 100% duty cycle (continuous wave) beam and lower duty cycles is made clear in Figure 9. Once the voltage is above approximately 60mV the force output is the same percentage of the continuous wave beam as its duty cycle. This makes sense, as the duty cycle represents the portion of the time that the beam is on (and thus able to impart a force).

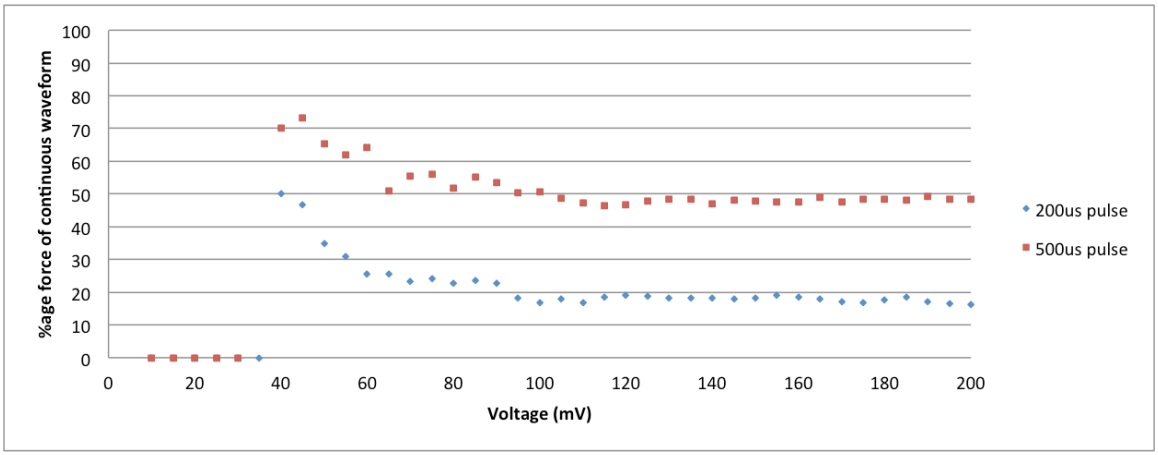

Figure 9: Percent of Continuous Wave load for Pulsed 1 MHz signal. The graph shows that the pulsed beams produced forces that correspond to their percent duty cycle. The 200us pulse width beam, which corresponds to a 20% duty cycle, produced roughly 20% of the force of the continuous wave. The same relation held for the 500us pulse width beam (50% duty cycle). These relations only became apparent above a noise floor of approximately 60-80mV.

In addition force output versus distance from target was measured for different voltage settings. This was done to determine how sensitive force measurements were to how precisely the target separation distance was set. As can be seen in the Figure10 below, while distance to target does affect measured force, the effect of selected voltage (which correlates to beam intensity) is more dramatic.

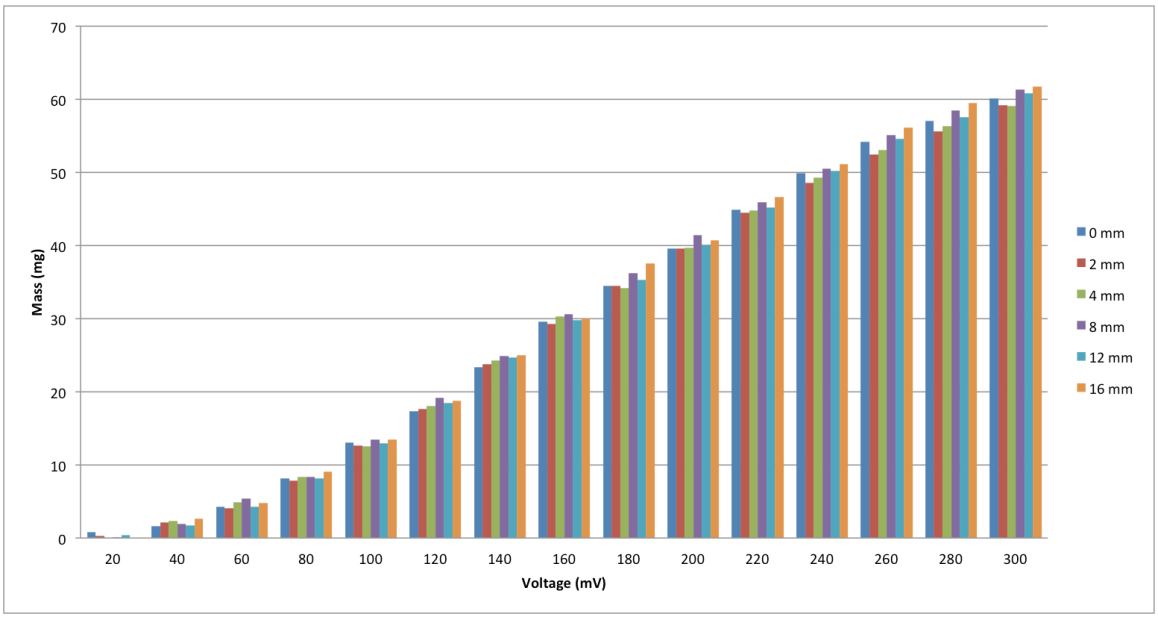

Figure 10: Graph of force verse input voltage for various transducer-to-cone distances with a 1MHz continuous wave. The graph shows that both transducer-to-cone distance and voltage are important variables for measured load. However, the variation of measured force from 0 mm to 16 mm (less than 8 mg for the larger voltages) is approximately the same variation achieved from a 20mV change in the input signal. The size of the variation of force measured at the lower voltages (below 120mV) was much less than the change between voltage intervals.

Measured force can be converted to beam intensity fairly easily[28].

$$p = Wgc$$

where:

$$W = measured\ force, grams$$
$$g = acceleration\ due\ to\ gravity, dynes$$
$$c = speed\ of\ propogation\ of\ sound, cm/sec$$
$$p = power, ergs/sec$$

This can be further simplified, assuming constant values for g and c. This yields the following equation[28]:

$$P = 14.65w$$

where:

$$P = power\ of\ ultrasound\ beam\ in\ watts$$
$$w = force\ of\ ultrasound\ beam\ in\ grams$$

From beam power we can convert to beam intensity (I) by dividing by the cross sectional area of the beam. Here we will assume that the cross sectional area is the same as the transducer (A= .25πD^2, D=.75"), which is a good approximation close to the source, as the beam has not yet diverged significantly. These calculations are useful for comparisons between ultrasound systems. From a cellular perspective, the beam intensity rather than total force produced by the beam is most comparable due to the small size of a cell relative to beam diameter. Beam Intensity, along with output relative to a 500mV continuous wave beam are summarized below in Table 3, for beam parameters used in Aims 2& 3.

Table 3: Comparison of measured and calculated ultrasound beam parameters (Load, Beam Intensity, and Beam Power) for input parameters (200mV and 500mV for 20%, 50%, and 100% duty cycle with 1MHz carrier and 1kHz pulse rate frequency) used for visualization experiments. Load was measured while beam intensity and beam power were calculated. Beam intensity is approximate due to assuming the cross sectional area of the beam is the same as the transducer cross sectional area (nominal .75" diameter).

Input Voltage	Duty Cycle	Load	Beam Intensity	Beam Power	% Output of 500mV CW
200mV	20%	8.3 mg	~11.8 mW/cm^2	121.9 mW	10.6%
	50%	22.2 mg	~31.4 mW/cm^2	325.2 mW	28.2%
	100%	42.7 mg	~60.5 mW/cm^2	625.6 mW	54.2%
500mV	20%	17.8 mg	~25.2 mW/cm^2	260.8 mW	22.6%
	50%	42.3 mg	~59.9 mW/cm^2	619.7 mW	53.7%
	100%	78.8 mg	~111.6 mW/cm^2	1154.4 mW	100%

5.2 Specific Aim 2: Mechanical Interaction with Scaffold

This set of experiments was aimed at visualizing the interaction of the physical force measured in Specific Aim 1 with a scaffold. The purpose of these experiments was to gain a greater understanding of how LIPUS interacts with ECM in vivo during clinical applications. This may help to optimize LIPUS applications, especially in conjunction with bone grafts and bone graft substitutes.

5.2.1 Beads in PuraMatrix

In this study the fluorescent beads were suspended in a 1% solution of PuraMatrix that was gelled on a glass slide. The hydrogel was then exposed to ultrasound of varying parameters and imaged using fluorescence microscopy. The beads were observed to move in a manner consistent with elastic compression of the matrix in which the beads were encapsulated. Specifically, the displacement was dependent on ultrasound parameters; in addition the beads returned to their initial position upon cessation of ultrasound exposure.

The effects of a 200mV 20% duty cycle LIPUS beam on the beads are seen in Figure 11. The boxed bead appears to move down approximately 1 bead diameter during 2 minutes of US exposure. During the 5 minutes of the recovery after exposure the bead appears to move 1 diameter back towards its original position.

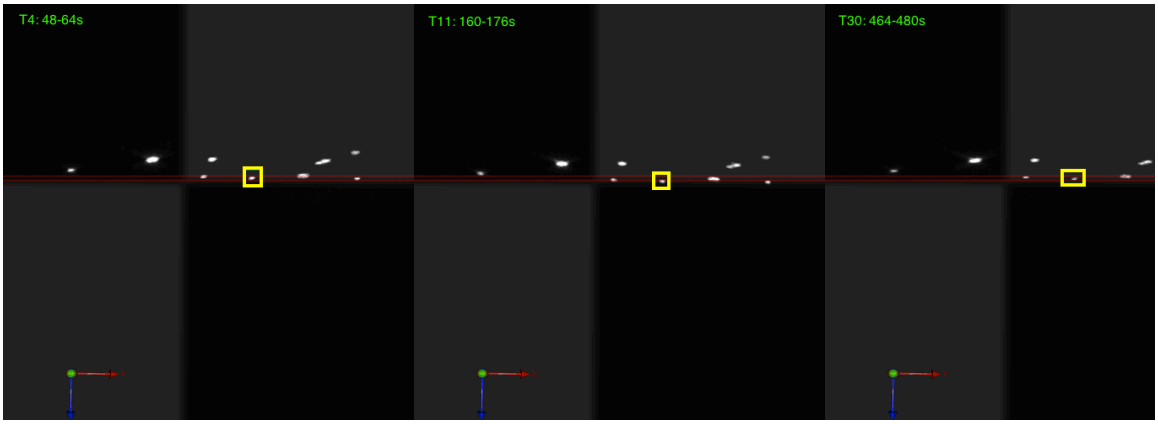

Figure 11: series of z-stacks of 1µm beads exposed to 200mV 20% duty cycle US; from left to right pre-US treatment (T4), just post-US (T11), full recovery ~5 minutes after US was discontinued (T30). The bead appears to move down .5 to 1 bead diameter under US exposure, and then recover the same amount after ultrasound was discontinued.

The effects of a 200mV 50% duty cycle LIPUS beam on the beads are seen in Figure 12. The boxed bead appears to move down approximately 2 bead diameters during 2 minutes of US exposure. During the 4 minutes of the recovery after exposure the bead appears to move 1 diameter back towards its original position.

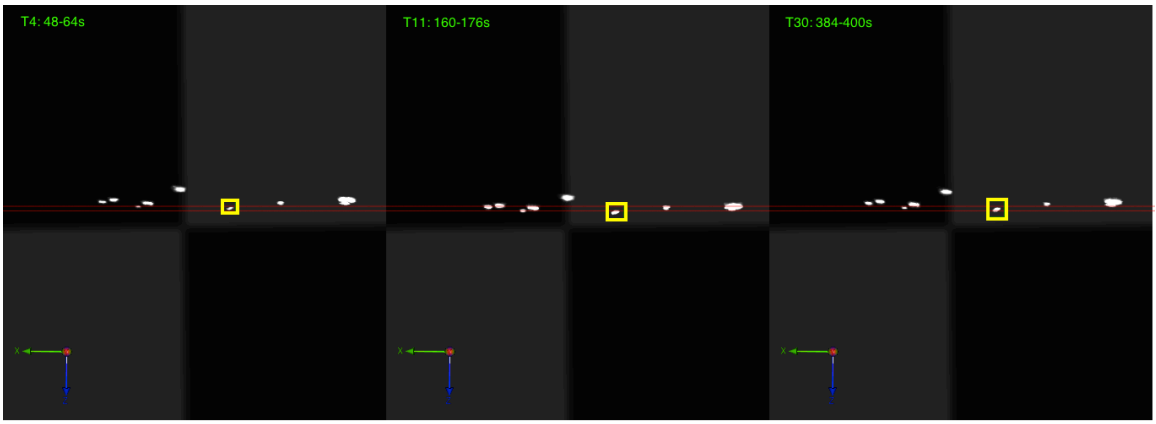

Figure 12: series of z-stacks of 1µm beads exposed to 200mV 50% duty cycle US; from left to right pre-US treatment (T4), just post-US (T11), full recovery ~4 minutes after US was discontinued (T30). The bead (cluster) appears to move down about 1 bead diameter and then recover slightly less than 1 bead diameter over a period of ~4 minutes of recovery.

The effects of a 200mV 100% duty cycle US beam on the beads are seen in Figure 13. The boxed bead appears to move down approximately 1 bead diameter during 2 minutes of US exposure. During the 5 minutes of the recovery after exposure the bead appears to move 1 diameter back towards its original position.

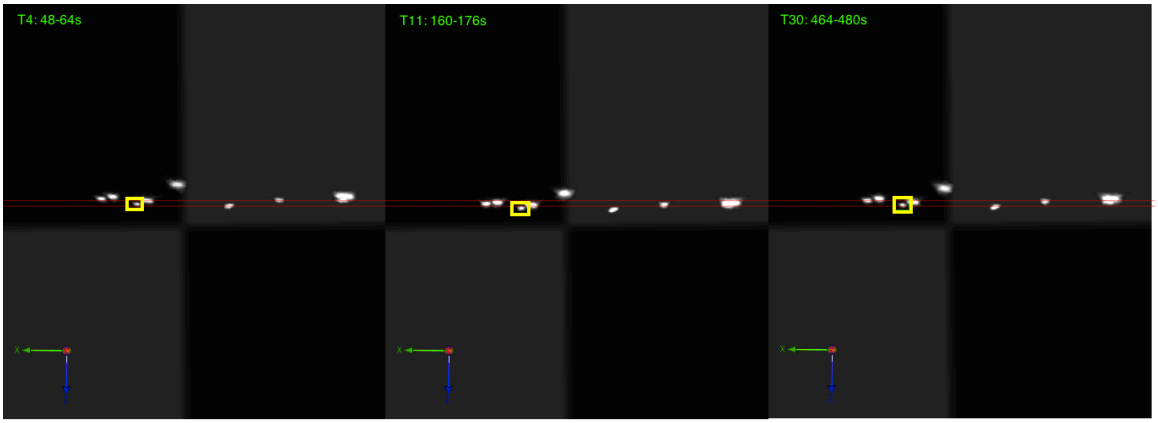

Figure 13: series of z-stacks of 1µm beads exposed to 200mV continuous wave US; from left to right pre-US treatment (T4), just post-US (T11), full recovery ~5 minutes after US was discontinued (T30).

The bead cluster appears to move slightly less than a whole bead diameter and then recover a distance of about half a cluster diameter after US was discontinued.

The effects of a 500mV 20% duty cycle LIPUS beam on the beads are seen in Figure 14. The boxed bead appears to move down approximately 3 bead diameters during 2 minutes of US exposure. During the 5 minutes of the recovery after exposure the bead appears to move 2 diameters back towards its original position.

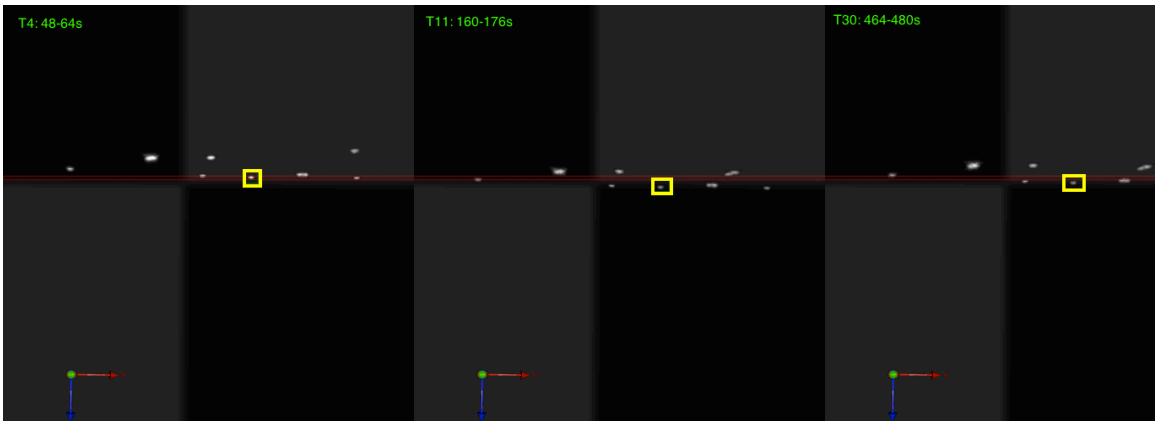

Figure 14: series of z-stacks of 1µm beads exposed to 500mV 20% duty cycle US; from left to right pre-US treatment (T4), just post-US (T11), full recovery ~5 minutes after US was discontinued (T30)

The effects of a 500mV 50% duty cycle LIPUS beam on the beads are seen in Figure 15. The boxed bead appears to move down approximately 4 bead diameters during 2 minutes of US exposure. During the 5 minutes of the recovery after exposure the bead appears to move 2 diameters back towards its original position.

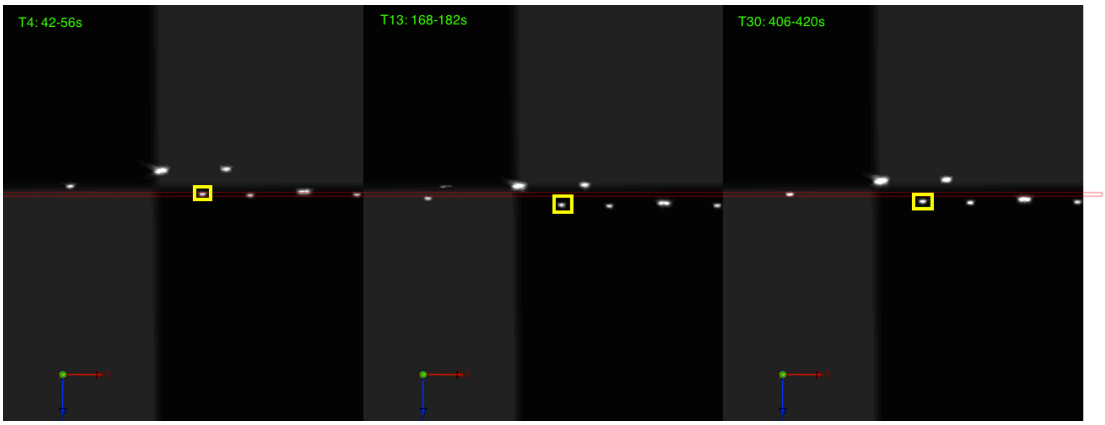

Figure 15: series of z-stacks of 1µm beads exposed to 500mV 50% duty cycle US; from left to right pre-US treatment (T4), just post-US treatment (T13), recovery ~4 minutes after US was discontinued (T30).

The effects of a 500mV 100% duty cycle US beam on the beads are seen in Figure 16. The boxed bead appears to move down approximately 5 bead diameters during 2 minutes of US exposure. During the 5 minutes of the recovery after exposure the bead appears to move 2 diameters back towards its original position.

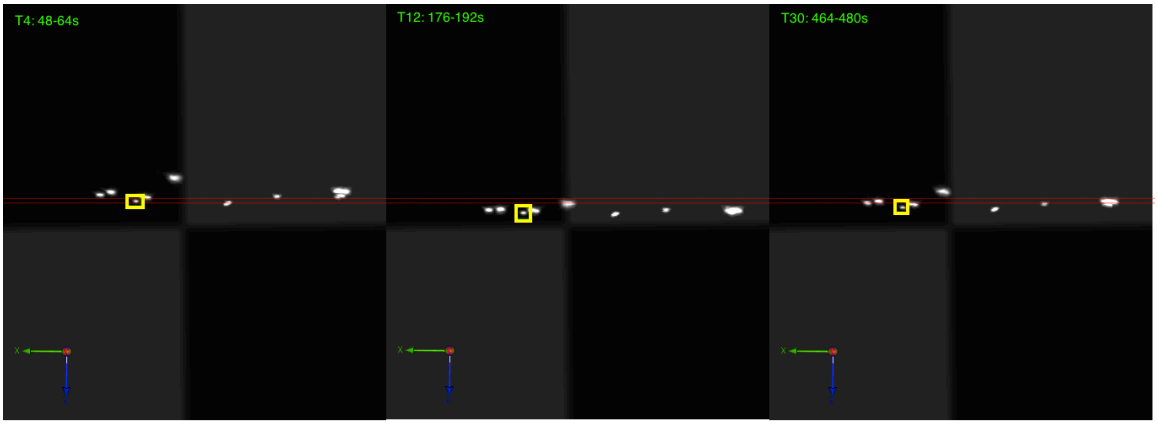

Figure 16: series of z-stacks of 1µm beads exposed to 500mV continuous wave US; from left to right pre-US treatment (T4), just post-US treatment (T12), recovery ~5 minutes after US was discontinued (T30).

As anticipated, the displacement of the beads appears to be proportional to the intensity of the ultrasound beam. Greater displacement occurred for higher intensity beams. Displacement parity for similar beam intensities, however, seems to be lacking. The qualitative displacement and relative beam intensities are summarized in Table 4.

Table 4: Comparison of Beam Intensity versus Bead Displacement

Input Voltage	Duty Cycle	Beam Intensity	Displacement [~ bead diameters]	% Output of 500mV CW
200 mV	20%	~11.8 mW/cm^2	1↓/1↑	10.6%
	50%	~31.4 mW/cm^2	2↓/1↑	28.2%
	100%	~60.5 mW/cm^2	1↓/1↑	54.2%
500mV	20%	~25.2 mW/cm^2	3↓/2↑	22.6%
	50%	~59.9 mW/cm^2	4↓/2↑	53.7%
	100%	~111.6 mW/cm^2	5↓/2↑	100%

5.3 Specific Aim 3: Mechanical Interaction with Cell

5.3.1 GFP-actin Macrophages on Glass

The purpose of the GFP macrophage on glass substrate experiments was to visualize the physical interaction of LIPUS with a cell. Previous results suggested that the cells are experiencing some sort of physical loading; these experiments were designed to see how such a load would physically affect the cells. In the side view of the cells in the figures 17-19, the cells can be observed to move down while exposed to ultrasound. The visible displacement is consistent with the idea that the cells are experiencing a nonzero unidirectional load concurrent

with the direction of beam propagation. The images also suggest that an actin response (areas of increased fluorescence) is occurring when the cells are subjected to ultrasound.

For the 500mV 20% duty cycle US beam the different states of exposure and recovery can be seen in Figure 17. The cell appears to move down slightly during US exposure. During recovery there are pronounced points of actin activity in the cell.

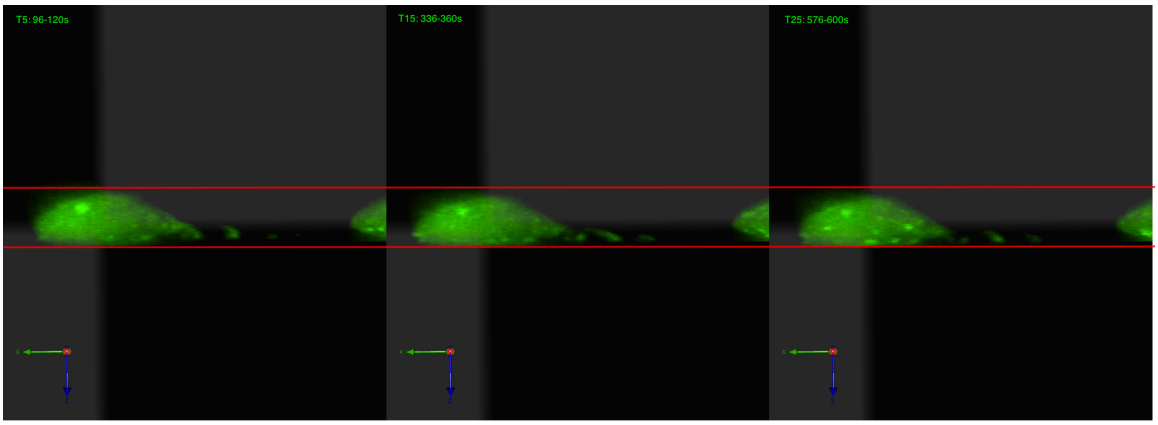

Figure 17: series of z-stacks for macrophage exposed to 500mV 20% duty cycle US; from left to right pre-US treatment (T5), just post-US (T15), recovery 4 minutes after US was discontinued (T25). The cell appears to flatten out slightly and move down slightly under US exposure. The majority of actin activity, as indicated by areas of increased fluorescence, occurs during recovery. This cell also had the most distinctly visible actin activity in the recovery phase.

For the 500mV 50% duty cycle US beam the different states of exposure and recovery can be seen in Figure 18. This cell experiences rather dramatic displacement, appearing to move down half of its height. In addition the cell appears to concentrate actin activity on the bottom of the cell as a result of US exposure as well as becoming more rectangular in shape and decreasing the

overall height of the cell. During recovery actin activity appears to shift to the top of the cell and is accompanied by a return to a more oblong rounded shape and an increase in cell height. The cell also returns to its original position level and shape during recovery.

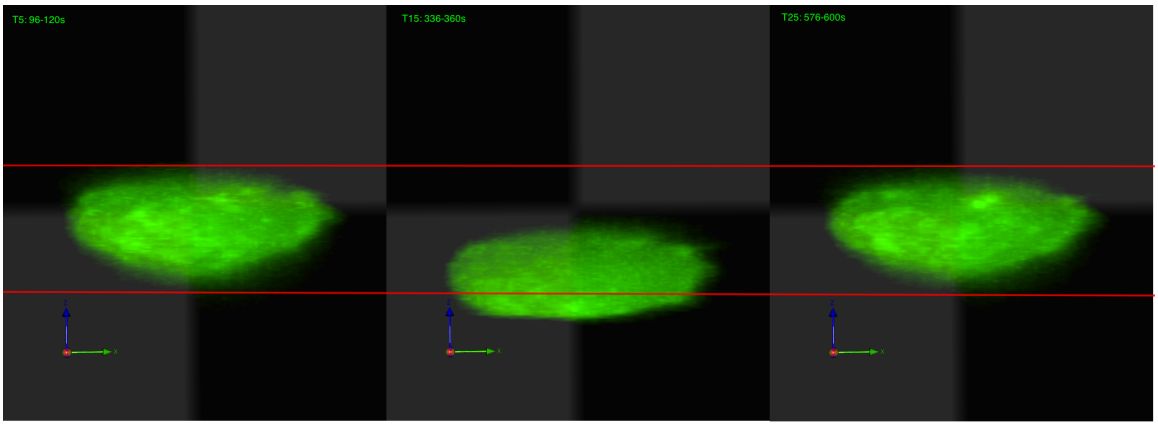

Figure 18: series of z-stacks for macrophages exposed to 500mV 50% duty cycle US; from left to right pre-US treatment (T5), just post-US (T15), recovery 4 minutes after US was discontinued (T25). The cell appears to move down close to half its height and more rectangular in shape under ultrasound. In addition, actin activity appears to be concentrated on the bottom of the cell during US exposure. During recovery the cell appears to return to a more rounded, oblong shape. In addition increased actin activity is seen on the top of the cell. This cell experienced the most dramatic displacement and deformation of the three examined.

For the 200mV, continuous wave US beam the different states of exposure and recovery can be seen in Figure 19. The cell appears to move down slightly during US exposure. The most pronounced of the subtle shift occurs in the cell process extended to the right of the cell. The cell then appears to recover its original position after US exposure has stopped.

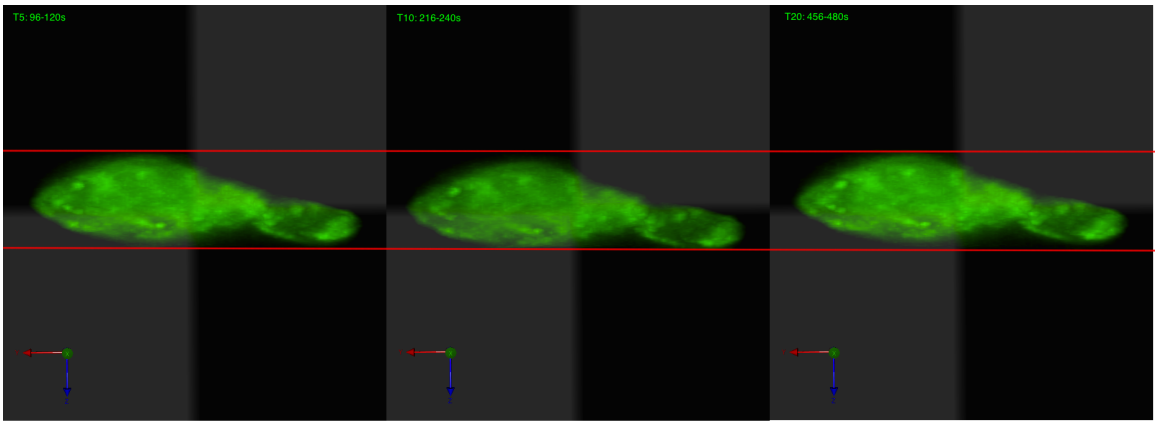

Figure 19: series of z-stacks for macrophage exposed to 200mV continuous wave US; from left to right pre-US treatment (T5), just post-US (T10), full recovery 4 minutes after US was discontinued (T20). Not much actin activity is visible, though the cell does appear to move down slightly during US exposure and then return to its original position during recovery. This lack of deformation and displacement is interesting because these settings have almost the same beam intensity as 500mV at 20% duty cycle (~60.5 mW/cm^2 vs ~59.9mW/cm^2); under these settings the cell moved about half of its height, in contrast to the barely perceptible movement under 200mV continuous wave.

Chapter 6: Discussion

Many studies have been done on the cellular signaling responses to ultrasound as well as the clinical outcomes of LIPUS therapy. However, the mechanism by which therapeutic ultrasound promotes fracture repair has remained poorly understood. This study was intended to partially investigate the mechanism, by looking into whether LIPUS produces an appreciable physical load on scaffolds and cells.

6.1 Specific Aim 1: System Characterization

In Specific Aim 1 it was shown that the constructed system could produce desired measurable intensities while adjusting a variety of LIPUS parameters (i.e. carrier wave frequency, duty cycle) with many other potential parameters which may also be adjusted (e.g. pulse rate frequency, carrier wave form). This system allows the free exploration of a variety of parameters while maintaining consistent beam intensity for comparison to 'standard' clinical ultrasound. Any variety of future set of parameters deemed to be of interest could be investigated without relying on commercially/clinically available LIPUS units. In addition, because the system is not donated by a corporate sponsor, the results are not subject to their approval prior to publication.

Furthermore, the system could even be adjusted to change parameters over the course of a study, to account for (and optimize in response to) changes in the behavior of cells and the properties of the fracture site / scaffold over the healing / ossification processes. Different stages of healing might benefit from local heating and be inhibited by the application of shear flow, while other stages may have opposite optimal parameters. Alternatively different types of fractures may benefit from different ultrasound parameters. This system has the flexibility to explore and accommodate all of these possibilities.

6.2 Specific Aim 2: Loading a Scaffold

In Specific Aim 2, it was shown that the beads in the scaffold could be moved 'remotely' (i.e. without physical contact) through the application of ultrasound, and that the beads would return to their original position after a period of recovery once the application of ultrasound had stopped. This suggests that the beads are embedded in the hydrogel, which is being compressed by the ultrasound. Further the return of the beads to their original position after the cessation of ultrasound suggests that the hydrogel is deforming elastically. An alternative explanation of this behavior is that the beads are merely buoyant and returning to their equilibrium level after the force applied to them (i.e. ultrasound) is removed. While this would be consistent with the beads returning to the same level, it does not explain returning to the same position. If the beads were buoyant rather than embedded more lateral motion would be expected than was observed.

From the preceding, we can assume that the measurable force of the ultrasound (see Aim 1) compressed the scaffold. Furthermore, the compression was proportional to the beam intensity, which corresponds to the applied force. This opens up a world of possibilities in terms of understanding how US works in current clinical applications and how it could be used (and optimized) in conjunction with natural and artificial bone grafts. There are several possible ways in which moving a scaffold could affect seeded/embedded cells. The cell could experience a shear stress / flow as the scaffold, on which the cell is attached, moves relative to the surrounding fluid. The cell could experience a

membrane strain as the substrate of the scaffold, on which the cell is attached, is stretched; or if the cell is attached to two strands it could stretch as the strands move relative to each other. In addition, if the cell is embedded within the scaffold, it might experience a compressive stress as the scaffold is compressed around it. These final two methods (essentially membrane strain mechanisms) seem most in agreement with current understanding of the principle mechanism for stimulating osteocytes in vivo. Because osteocytes are derived from osteoblasts which have become embedded in (partially ossified) ECM this model may stimulate similar results.

Furthermore, if a scaffold is placed in a defect, the interaction with LIPUS could be tuned to take advantage of these different mechanisms. Either the properties of the scaffold could be adjusted (in the case of a bone graft substitute) or the output parameters of the LIPUS could be adjusted, in order to optimize and investigate the fracture repair. Changes in the mechanical properties of the scaffold could be tracked over time during the healing process (e.g. as a result of ossification of collagen fibers). Different types of scaffold could be tested to see how they respond to LIPUS in terms of deformation, as well as how different LIPUS parameters affect deformation. Additionally, the mechanical responses of different stages of fracture repair could be examined, as well as why different stages of fracture repair have differently levels of benefit from LIPUS in terms of deformation.

6.3 Specific Aim 3: Loading a Cell

In Specific Aim 3, ultrasound was used to apply a physical load to a cell. This was observed through visualization of vertical displacement and deformation of the cell during the application of ultrasound followed by the return of the cell to roughly its pre-exposure position. This is consistent of with the idea that a force physically displaced the cell. However, what is not clear is whether the observed displacement and deformation was the result of a purely mechanical mechanism (i.e. displacement caused by the force of the ultrasound on the cell membrane) or an active response by the cell (either inhibiting more extreme displacement or amplifying the effect). What is also unresolved is whether the observed displacement or deformation is important in clinical outcomes. However, what is clear is that physical displacement and deformation occurred in response (whether directly or not) to exposure from ultrasound, and was reversed when exposure stopped.

Alternative methods of making the cells fluorescent were attempted. One such attempt was to use a dye that becomes fluorescent when it encountered peptides inside of cell, with the purpose of being able to have dye outside of the cell that did not produce background fluorescence. In retrospect this was a poor dye choice in a system that involved a peptide hydrogel; it did however, illustrate potential problems with attempting to visualize a wholly stained scaffold or staining a cell after it has been embedded in the scaffold. Here the problem encountered was that the entire scaffold fluoresced, masking both the individual

strands of the scaffold and the cells, which the dye was intended to stain. This further illustrates why using GFP expressing cells is advantageous: there are no unintended side of effects of fluorescent dyes staining things that weren't the target.

6.4 Tying It All Together

To reiterate: In Specific Aim 1 it was shown that almost any combination of US parameters along with known beam intensity could be produced. In Specific Aim 2 it was shown that US can remotely deform a scaffold. In Specific Aim 3 it was shown that US can remotely displace and deform a cell. Together a known load with an arbitrary array of parameters can be applied to deform and displace a cell in a scaffold. This is the most obvious next step of investigation, especially because it more closely resembles in vivo conditions than those investigated so far. This will allow greater understanding of the mechanisms by which current clinical LIPUS works and future tuning for better, potentially non-invasive, fracture repair. More specifically, the deformation and displacement of a cell relative to the scaffold in which it is embedded could be investigated.

Chapter 7: Future Work

There are several clear directions in which this work may be continued. First, GFP osteoblasts (and other bone cell types) could be substituted for GFP macrophages. Bone cells would clearly give greater insight into how ultrasound affects bone cells in vivo compared to macrophages. Further, cells, rather than

beads could be embedded in the hydrogel. Both of these steps would create a greater understanding of how LIPUS interacts with cells in vivo. In addition, a study could compare the response of regular (GFP) bone cells with ones that lack certain mechanotransduction capabilities. This could help distinguish whether the deformation and displacement observed in normal cells is purely a mechanical response to forces on the membrane of the cell or if an active biological response is involved.

Another direction for further investigation would be to follow changes in response of cells over time. For instance, the cells could be exposed to 20-minute daily US sessions (similar to clinical applications) and then the physical response could be gauged for different time points (e.g. day 1, 2, 3, 7, 14, etc). In parallel, studies could measure protein expression and degree of ossification of the ECM and correlate these to changes in physical response to ultrasound.

References

1. Bartel, Donald L, Dwight T Davy, and Tony M Keaveny. 2006. *Orthopaedic Biomechanics*. Pearson Prentice Hall.
2. Hughes, Sean, and Ian McCarthy, eds. 1998. *Sciences Basic to Orthopaedics*. WB Saunders Company Limited.
3. Einhorn, T.A., Regis J. O'Keefe, and J.A. Buckwalter. 2006. *Orthopaedic Basic Sciences: Foundations of Clinical Practice*. 3rd ed. American Academy of Orthopaedic Surgeons.
4. Burger, E H, and J Klein-Nulend. 1999. Mechanotransduction in bone--role of the lacuno-canalicular network. *The FASEB journal : official publication of the Federation of American Societies for Experimental Biology* 13 Suppl (January): S101-12. http://www.ncbi.nlm.nih.gov/pubmed/10352151.
5. Browne, Patrick S H. 1983. *Basic Facts of Fractures*. Hong Kong: Blackwell Scientific Publications.
6. Cobbold, Richard S C. 2007. *Foundations of Biomedical Ultrasound*. 1st ed. New York: Oxford University Press.
7. Rayleigh, John William Strutt. 1877 & 1878. *The Theory of Sound, Vols. I & II*. London: MacMillan Co.
8. Blackstock, David T. 2000. *Fundamentals of Physical Acoustics*. New York: Wiley.
9. Claes, Lutz, and Bettina Willie. 2007. The enhancement of bone regeneration by ultrasound. *Progress in biophysics and molecular biology* 93, no. 1-3 (January): 384-398. doi:10.1016/j.pbiomolbio.2006.07.021.
10. Wolff, Julius. 1892. *The Law of Bone Remodelling (Das Gesetz der Transformation der Knochen, Hirschwald)*. Berlin: Springer.
11. Frost, Hm. 2004. A 2003 Update of Bone Physiology and Wolff's Law for Clinicians. *The Angle Orthodontist* 74, no. 1: 3-15. http://www.ncbi.nlm.nih.gov/pubmed/15038485.
12. Weidman, Judith. 2010. Effects of Low Intensity Pulsed Ultrasound and Low Level Heat on Bone Cells. *Theses and Dissertations*. Ryerson University, Toronto. http://digitalcommons.ryerson.ca/dissertations/131/.
13. Orr, A Wayne, Brian P Helmke, Brett R Blackman, and Martin A Schwartz. 2006. Mechanisms of mechanotransduction. *Developmental cell* 10, no. 1 (January): 11-20. doi:10.1016/j.devcel.2005.12.006. http://www.ncbi.nlm.nih.gov/pubmed/16399074.
14. Wang, James Hc, and Bin Li. 2010. Mechanics rules cell biology. *Sports medicine, arthroscopy, rehabilitation, therapy & technology : SMARTT* 2, no. 16 (January): 1-7. doi:10.1186/1758-2555-2-16. http://www.pubmedcentral.nih.gov/articlerender.fcgi?artid=2912251&tool=pmcentrez&rendertype=abstract.
15. Murray, D W, and N Rushton. 1990. The effect of strain on bone cell prostaglandin E2 release: a new experimental method. *Calcified tissue international* 47, no. 1 (July): 35-9. http://www.ncbi.nlm.nih.gov/pubmed/2369689.
16. Neidlinger-Wilke, C, I Stalla, L Claes, R Brand, I Hoellen, S Rübenacker, M Arand, and L Kinzl. 1995. Human osteoblasts from younger normal and osteoporotic donors show differences in proliferation and TGF beta-release in response to cyclic strain. *Journal of biomechanics* 28, no. 12 (December): 1411-8. http://www.ncbi.nlm.nih.gov/pubmed/8666581.
17. Buldakov, Mikhail A., Mariame A. Hassan, Qing-Li Zhao, Loreto B. Feril Jr., Nobuki Kudo, Takashi Kondo, Nikolai V. Litvyakov, et al. 2009. Influence of changing pulse repetition frequency on chemical and biological effects induced by low-intensity ultrasound in vitro. *Ultrasonics Sonochemistry* 16, no. 3 (March): 392-397. doi:10.1016/j.ultsonch.2008.10.006. http://www.sciencedirect.com/science/article/B6TW3-4TPF4P2-6/2/29b7a936e529ccc3fa5ccb708cc6f2cf.
18. Eckart, Carl. 1948. Vortices and Streams Caused by Sound Waves. *Physical Review* 73, no. 1
19. Duck, Francis A. 1998. Ultrasound in medicine :- Chapter 3, radiation pressure and streaming. In *Ultrasound in Medicine*, ed. Francis A. Duck, A. C. Baker, and H.C. Starritt, 39-56. 1st ed. Taylor & Francis.

20. Duck, Francis A. 2002. Nonlinear acoustics in diagnostic ultrasound. *Ultrasound in Medicine & Biology* 28, no. 1 (January): 1-18. doi:10.1016/S0301-5629(01)00463-X. http://www.sciencedirect.com/science/article/B6TD2-458P95W-1/2/3f479e37d54ca61a62252b7fcbb23c2b.
21. Duck, Francis A. 2008. Hazards, risks and safety of diagnostic ultrasound. *Medical Engineering & Physics* 30, no. 10 (December): 1338-1348. doi:10.1016/j.medengphy.2008.06.002.
22. Starritt, H.C., Francis A. Duck, and Victor F. Humphrey. 1989. An experimental investigation of streaming in pulsed diagnostic ultrasound beams. *Ultrasound in Medicine & Biology* 15, no. 4: 363-373. doi:10.1016/0301-5629(89)90048-3. http://www.sciencedirect.com/science/article/B6TD2-4BP8CG4-21/2/db482e72284c60f9be9971d92a014cc6.
23. Starritt, H.C., Francis A. Duck, and Victor F. Humphrey. 1991. Forces acting in the direction of propagation in pulsed ultrasound fields. *Physics in Medicine and Biology* 36, no. 11 (November): 1465-1474. http://www.ncbi.nlm.nih.gov/pubmed/1754617.
24. Torr, G. R. 1984. The acoustic radiation force. *American Journal of Physics* 52, no. 5 (May): 402. doi:10.1119/1.13625. http://link.aip.org/link/?AJP/52/402/1&Agg=doi.
25. Harris, Gerald, and Robert Phillips. 2008. Information for Manufacturers Seeking Marketing Clearance of Diagnostic Ultrasound Systems and Transducers. http://www.fda.gov/downloads/MedicalDevices/DeviceRegulationandGuidance/GuidanceDocuments/UCM070911.pdf.
26. Sakai, Stacie Sachiko. 2003. Radiation force measurements at a water-air interface. *Theses and Dissertations*. University of Illionois, Urbana-Champaign. ttp://www.brl.uiuc.edu/Downloads/.
27. Palumbo, Vincent. 2010. Combined Atomic Force Microscopy and 3-D Optical Investigation of the Active Cytoskeletal Response of Living MH-S Cells to Nanoscale Structures and Forces. *Theses and Dissertations*. University of Connecticut.
28. Alberts, Bruce, Alexander Johnson, Julian Lewis, Martin Raff, Keith Roberts, and Peter Walter. 2007. *Molecular Biology of the Cell*. 5th ed. Garland Science.
29. 3DM. PuraMatrix Characteristics & Comparison.
30. Athanasiou, K a, C Zhu, D R Lanctot, C M Agrawal, and X Wang. 2000. Fundamentals of biomechanics in tissue engineering of bone. *Tissue engineering* 6, no. 4 (August): 361-81. doi:10.1089/107632700418083. http://www.ncbi.nlm.nih.gov/pubmed/10992433.
31.